Hygrothermal Aging and Fracture Behavior of Styrene-Acrylonitrile/Acrylate Based Core–Shell Rubber Toughened Poly(butylene terephthalate)

Z. A. MOHD ISHAK,[1] U. S. ISHIAKU,[1] J. KARGER-KOCSIS[2]

[1] School of Industrial Technology, Universiti Sains Malaysia, 11800 Pulau Pinang, Malaysia

[2] Institute for Composite Materials, University of Kaiserslautern, P.O. Box 3049, D-67663 Kaiserslautern, Germany

Received 2 September 1998; accepted 15 May 1999

ABSTRACT: A study of hygrothermal aging in terms of the kinetics of moisture absorption by poly(butylene terephthalate) (PBT) and styrene-acrylonitrile/acrylate based core–shell rubber (CSR) toughened PBT (PBT-CSR) was undertaken. The diffusion of water into the PBT compounds with various CSR contents was investigated by immersion of specimens in water at temperatures between 30 and 90°C. It was observed that the equilibrium moisture content and the diffusion coefficient of the PBT both increased with increasing CSR content. The fracture behaviors of the PBT and PBT-CSR were investigated. The focus of investigation was on the effect of an internal parameter (rubber content) and external parameters (testing temperature, deformation rates, and hygrothermal aging) on the fracture behavior of these materials. The fracture response of the various materials was evaluated by the fracture toughness and energy measured on static-loaded compact tension specimens. The tensile and fracture behavior of PBT and PBT-CSR was affected by both the internal and external parameters. On its own the CSR impact modifier failed to improve the toughness of PBT at either high testing speed or subambient temperature (−40°C). Based on the dynamic mechanical analysis study, the CSR is believed to behave as a rigid particulate filler in the PBT that consequently reduces the ductility of the PBT. All the materials tested showed poor retention of the tensile and fracture properties upon exposure to hygrothermal aging at 90°C, and these properties could not be restored by subsequent drying. This was attributed to severe hydrolytic degradation of the PBT that caused permanent damage to the materials. The failure modes of PBT and PBT-CSR were assessed by fractographic studies in a scanning electron microscope. J Appl Polym Sci 74: 2470–2481, 1999

Key words: fracture; core–shell impact modifiers; hygrothermal aging; rubber toughened; poly(butylene terephthalate)

INTRODUCTION

Poly(butylene terephthalate) (PBT) is a semicrystalline polyester that has been used as an engineering thermoplastic since the early 1970s. It possesses good thermal, chemical, physical, and mechanical properties, combined with satisfactory processing characteristics.[1] However, it has two main disadvantages: it has limited toughness at high deformation rates and at low temperatures, and it has a strong tendency to undergo hydrolysis that leads to serious embrittlement when subjected to hygrothermal aging. In a re-

Correspondence to: Z. A. Mohd Ishak.

Contract grant sponsor: German Science Foundation; contract grant number: Ka-1202/3-1.

Journal of Applied Polymer Science, Vol. 74, 2470–2481 (1999)
 CCC 0021-8995/99/102470-12

cent study Mohd Ishak and Lim[2] reported that hydrolysis, which became more prominent in a hot and wet environment, resulted in the formation of microvoids and the absence of a plastic deformation process. Thus, research and development efforts have been devoted to solving these acute problems. Attempts to enhance the fracture behavior of PBT by the addition of elastomeric impact modifiers (IMs) have resulted in the commercial development of several types of rubber toughened PBTs (RTPBTs). Core–shell impact modifiers consisting of a rubbery core (usually a copolymer based on either butadiene or acrylate) and a hard shell such as styrene-acrylonitrile (SAN) or poly(methylmethacrylate), as well as functionalized polyolefins and thermoplastic elastomers, are used to impact modify PBT.[3–5] It has been found that the toughness is related to the rubber content, types of rubber, particle size of the rubber, interparticle distance, and rubber particle cavitation behavior. A recent study reported that the irregularity in the shape of the butadiene-*co*-AN rubbers in PBT/nitrile rubber blends is also effective in reducing the shear yield stress of the polyester matrix.[6] Several mechanisms were proposed to explain the toughness increment; these include multiple crazing, shear yielding, crazing with shear yielding, cavitation, and rubber particle stretching and tearing.[7] However, the relative contribution of each mechanism toward toughness enhancement and the sequence of toughening processes is still debatable.

This article reports on hygrothermal, tensile, and fracture behaviors of PBT and PBT-core–shell rubber (CSR). The aim is to investigate the effects of internal parameters (such as rubber content) and external parameters (such as testing speed and temperature). As mentioned earlier, PBT is known to possess moderate stability to hydrolysis. Although some hygrothermal aging studies have been conducted on PBT,[2,8] PBT/polycarbonate blends,[9] and short glass fiber (SGF) PBT,[2] there are only a limited number of research works that have been published for RTPBTs and their related composites. Recently Czigany et al.[10] and Mohd Ishak et al.[11] reported on the effects of hygrothermal aging on the fracture behavior of SGF-reinforced, toughened PBT composites. They noted that the combination of SGF with various types of IMs produced a synergistic effect in terms of enhancing the retentionability and recoverability of the fracture properties of the RTPBT composites under such an adverse condition. This article focuses on two main issues related to hygrothermal aging. First, we report on the hygrothermal aging experiments that were conducted through the study of the kinetics of moisture absorption. The effects of immersion temperatures and rubber content on the diffusion coefficient and equilibrium moisture content were determined. Second, the effects of hygrothermal aging on the tensile and fracture properties of RTPBT are discussed.

EXPERIMENTAL

Materials

Neat PBT and CSR-modified PBT (PBT-CSR) containing 10, 20, and 30 wt % of an acrylate based CS-type modifier dispersed in a SAN matrix (CSR) were supplied by BASF AG. Scanning electron microscopic (SEM) investigations found the mean particle size of the CSR modifiers to be about 1 μm.

Processing

These materials were injection molded on a Rico 210/160 HT injection molding machine at melt and mold temperatures of 260 and 80°C, respectively, in film-gated 180 $\times$ 190 $\times$ 4 mm rectangular plaques.

Dynamic Mechanical Thermal Analysis (DMTA)

Rectangular specimens of about 60 $\times$ 10 mm^2 were cut from the gauge of the L-shaped dumbbells (cf. Fig. 1) and subjected to load-controlled sinusoidal loading in an Eplexor 150-N DMTA device (Gabo Qualimeter, Ahlden, Germany). Measurements occurred in tensile mode (static and oscillating loads of 50 and 25 N, respectively; clamped length = 50 mm) at a frequency of 10 Hz. The composites' viscoelastic properties [i.e., the complex dynamic modulus (E^*)] and the mechanical loss factor tan δ (tan $\delta = E''/E'$, where E'' and E' are the loss and storage modulus, respectively, and $E^* = E' + iE''$ holds) were evaluated in the temperature range of -100 to $+250$°C.

Kinetics of Moisture Absorption

The specimens were dried at 100°C over silica gel in a vacuum oven at 80°C for 12 h prior to immersion in distilled water in thermostated vessels at 30, 60, and 90°C. Weight gains after exposure were recorded by removal of the specimens from the environment and by weighing them periodi-

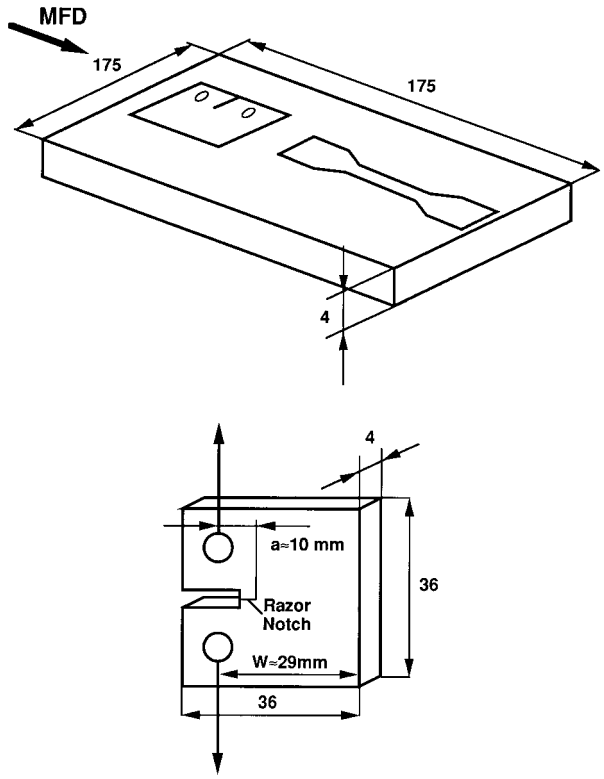

Figure 1 Machining and designation of the tensile and CT specimens.

cally on a Mettler AT 261 balance with a precision of 1 mg.

The percentage gain at any time t as a result of moisture absorption was determined by

$$M_t\,(\%) = (W_w - W_d)/W_d \times 100 \qquad (1)$$

where W_d and W_w denote, respectively, the weight of the dry material (i.e., the initial weight of the material prior to exposure to the environment) and the weight of the moist material. The percentage of the equilibrium moisture absorption, M_m, was calculated as an average value of several consecutive measurements that showed no appreciable additional absorption.

The weight gain resulting from moisture absorption can be expressed in terms of two parameters, the diffusion coefficient or diffusivity, D, and the maximum moisture content, M_m, as[12]

$$\frac{M_t}{M_m} = 1 - \frac{8}{\pi^2}\exp\left[-\left(\frac{Dt}{h^2}\right)\pi^2\right] \qquad (2)$$

where t is the time and h is the thickness of the specimen.

Tensile Test

Tensile specimens in accordance with ASTM D638 type 1 were machined from the molded plaques using a high speed specimen cutter (Cutvis model, Ceast, Italy). Specimens were cut parallel or longitudinal (L) to the mold filling direction (MFD) as shown in Figure 1. Tensile properties (tensile strength and tensile strain) were determined with a Zwick 1445 type testing machine at 20°C with a crosshead speed of 1 mm/min. Five specimens of each materials were tested.

Fracture Toughness

Compact tension (CT) specimens (notch length, $a \sim 10$ mm; free ligament width, $W = 29$ mm) were machined from the injection molded plaques as shown in Figure 1. Specimens with an initial notch cut transverse to the MFD were designated as L-T according to the ASTM E 616-81 standard. Thus, in the L-T CT specimens, their loading occurred longitudinal to the MFD. Prior to the static loading tests the notch of the CT was sharpened with a fresh razor blade.

Fracture toughness determinations were performed on a Zwick 1445 testing machine. Measurements conducted at different temperatures (−60, 20, and 80°C) were achieved by the use of a thermostatically controlled chamber attached to the testing machine. A crosshead speed, v, of 1 mm/min was used throughout. At 20°C additional tests were performed at a crosshead speed of 1000 mm/min to investigate the effect of testing speed. The fracture toughness (K_c) and fracture energy (G_c) were calculated in accordance with the recommendation of the protocol of the ESIS TC-4. In all cases, five CT specimens of each materials were tested.

Conditioning of Specimens

Because of the hygroscopic nature of PBT, the machined tensile and CT specimens were placed in a vacuum oven at 100°C for 48 h prior to testing. Upon removal from the oven the specimens were allowed to cool to room temperature inside a desiccator; these specimens are then regarded to be in the as-received (AR) state.

The study on the effect of water uptake on the tensile and fracture properties was also carried out on PBT and PBT-CSR. The specimens were hygrothermally aged (HA) at 30, 60, and 90°C. Once the water uptake in the specimens reached a saturation limit, tensile and fracture tests were

both carried out at room temperature using a crosshead speed of 1 mm/min.

The recovery of the tensile and fracture properties was studied on redried specimens (RD); redrying of the specimens occurred in a vacuum oven at 100°C for 48 h. Testing of the RD specimens was conducted under the same conditions used in the AR and HA states.

Fractography

The failure mode of the fractured CT specimens was examined using a Jeol JSM 5400 scanning electron microscope. SEM micrographs were taken at a 25-kV acceleration voltage at various magnifications. Prior to the SEM observations the fractured parts were mounted on aluminum stubs and sputter coated with a thin layer of gold to avoid electrical charging during examination.

RESULTS AND DISCUSSION

Kinetics of Moisture Absorption

Figure 2 shows the percentage moisture absorption, M_t, of PBT and PBT-CSR as a function of $t^{1/2}$ at an immersion temperature of 60°C. The initial linear relationship between M_t and $t^{1/2}$ was clearly observed in each case, followed by saturation. This indicates that Fickian behavior was observed.

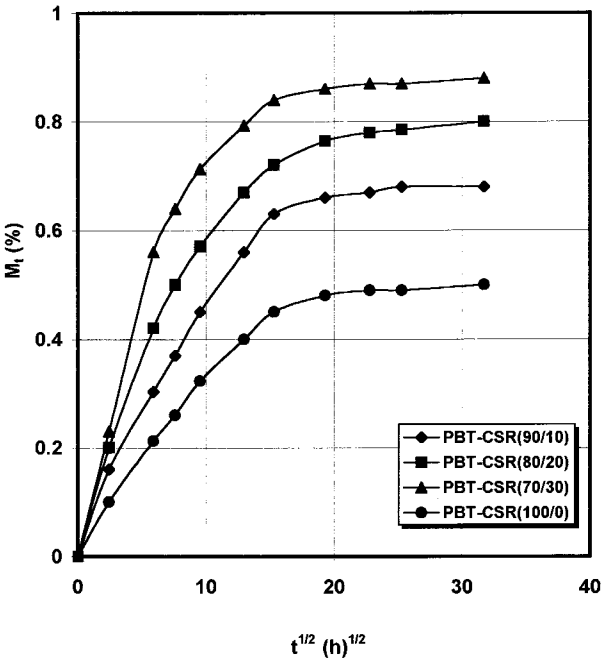

Figure 2 Moisture uptake of PBT and PBT-CSR at 60°C.

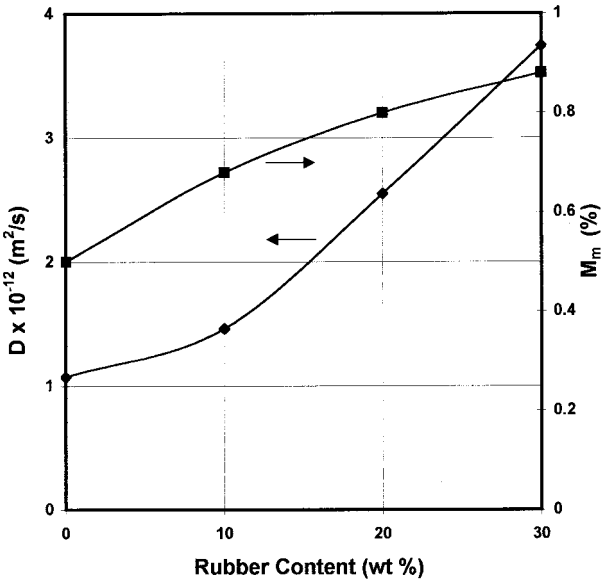

Figure 3 Variation of diffusion coefficient, D, and maximum moisture content, M_m, with CSR rubber content.

The diffusion coefficient D can be calculated from the initial linear portion of the absorption curve as[2]

$$M_t = M_m\left[\left(\frac{4}{h}\right)\left(\frac{D}{\pi}\right)^{1/2} t^{1/2}\right] \tag{3}$$

where M_t is the amount of moisture absorbed at time t, M_m is the maximum moisture content, and h is the thickness of the sample.

Figure 3 shows the effect of CSR loading on the values of D and M_m. The value of M_m for PBT is in agreement with the range of values reported by Mohd Ishak and Lim.[2] The figure also indicates that PBT-CSR absorbed considerably more moisture than PBT and the values of M_m increase with increasing CSR content. This is obviously related to the presence of CSR impact modifiers. The SAN that formed the shell of the CSR is known to be a hygroscopic polymer, and it has been reported that it can absorb up to 0.4% of moisture.[13] In addition, there is also a tendency for the acrylate rubber forming the core of the CSR to absorb moisture because polyacrylates are known to be hygroscopic materials.[14] The steady increase in D with increasing CSR content shown in the same figure also seems to indicate that the presence of CSR changed the microstructures of the PBT matrix in that it permitted the diffusion

of water molecules to take place at a faster rate. There is a possibility that the interfacial adhesion between CSR and PBT may also influence the nature of the moisture uptake. In the fiber-reinforced plastics, for instance, the interfacial damage was found to be one of the main factors responsible for the enhancement of moisture penetration into the composites.[2,11,12] The values of the diffusion coefficients obtained in the present study are in agreement with the range of values reported by other workers for most polymers.[12]

Effect of Rubber Content

Figure 4 shows the effect of the CSR rubber content on the tensile strength and tensile strain of PBT. As expected, the incorporation of CSR modifiers resulted in a continuous drop in tensile strength of the PBT matrix. At 30 wt % rubber content the tensile strength of the PBT dropped by about 25%. This clearly indicates that the presence of flexible, low strength rubber particles contributed adversely to the strength of the PBT. In fact, similar trends were also observed by several other researchers on different toughened thermoplastics blends.[15,16] The incorporation of about 20 vol % of finely dispersed ethylene propylene diene monomer rubber particles into nylon 6,6 reduced the tensile strength of the nylon 6,6 matrix from 80 to about 50 MPa.[17] As for the tensile strain, the trend shown in Figure 4 is rather unexpected. The addition of CSR modifiers did not improve the tensile strain of the PBT. Because tensile strain is an indirect indication of toughness, it can be inferred that there is no enhancement in the toughness of PBT upon the incorporation of CSR rubber particles. The drastic drop in tensile strain with the addition of 20 wt % CSR (i.e., to a lower value than that of neat PBT) seems to indicate that the CSR rubber particles are not behaving as a toughening agent but instead are behaving as rigid particles that restrained matrix deformation. Consequently, they inhibit the formation of a large damage zone, which is an important requirement for high toughness. This remark will be further supported by the fracture toughness data that will be discussed later.

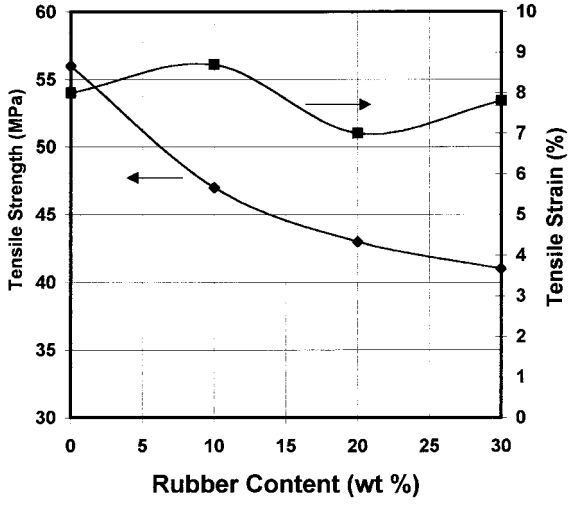

Figure 4 The effect of CSR rubber content on the tensile strength and tensile strain of PBT.

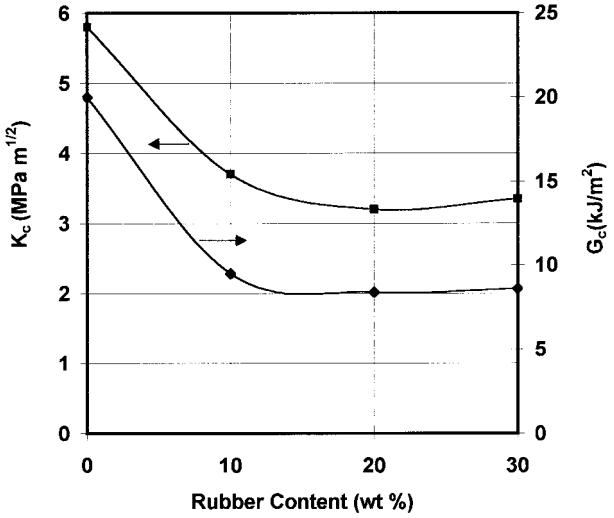

Figure 5 The variation of K_c and G_c with CSR rubber content.

Figure 5 shows the variation of K_c and G_c with rubber content. Both fracture parameters dropped sharply with the initial incorporation of 10 wt % CSR modifiers. Further additions of rubber modifiers did not give any positive contribution toward enhancing the toughness of the PBT matrix. This trend confirms our earlier observation on the variation of tensile strain with CSR content. According to two groups,[18,19] in rubber toughened thermoplastics, high fracture toughness is attributed to the formation of a large stable damage zone. Rubber particles stabilize the damage zone through multiple craze and shear-band initiation associated with cavitation. This function is then related to several factors such as the rubber content, type of rubber, particle size of the rubber, distribution of rubber particles, and interparticle distance, as well as rubber particle cavitation behavior. Rubber cavitation and the sequence of cavitation play a significant role in encouraging shear deformation. In the present context the poor toughening behavior of CSR modifiers is believed to have originated from

the nature of the rubber particles. As mentioned earlier, CSR is an acrylate based CS-type modifier dispersed in a SAN matrix. Because SAN is known to consist of a relatively rigid molecular structure, it has the tendency to suppress the elastomeric contribution of the acrylate modifiers. Thus, the low fracture strength and the inability to form a stable damage zone during the fracture process could account for the poor fracture properties of PBT-CSR. This subject will be dealt with in detail in the following section.

Effect of Temperature

Figure 6 shows the variation of K_c with temperature for PBT and PBT-CSR (W_r = 20 wt %). It can be seen that, irrespective of the testing temperature, the former has higher K_c values than the latter, albeit the difference in the values is more significant at subambient. At 20°C the K_c value of about 5.8 MPa $m^{1/2}$ for PBT clearly indicates that it is a ductile material. This is not surprising because the presence of plastic deformation in the form of matrix tearing, shear yielding, and crazing is apparent from the SEM micrograph of the fractured specimen. This subject will be discussed in detail later.

At a testing temperature of −40°C there is no sign of embrittlement of PBT. This may be attributed to the presence of a secondary relaxation that tends to flexibilize the materials at lower

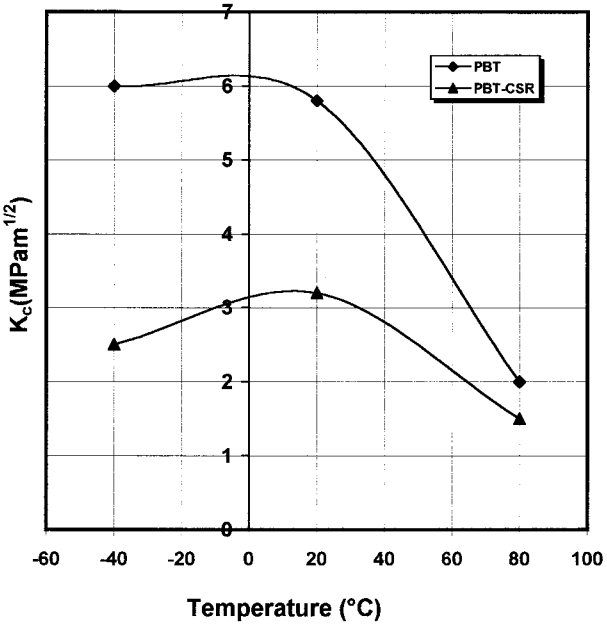

Figure 6 The effect of testing temperatures on the K_c of PBT and PBT-CSR (W_r = 20 wt %).

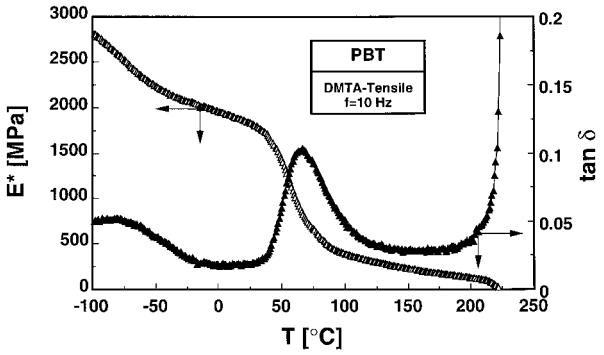

Figure 7 Variation of E^* and tan δ with temperature for PBT.

temperature. From the plot of loss modulus E^* and tan δ versus temperature (see Fig. 7) it can be seen that PBT displays a secondary transition at about −80°C. Thus, when the test was conducted at −40°C the mobility of the chains tended to increase the energy absorbing capabilities of the PBT. Consequently, PBT is able to retain its toughness at subambient temperatures. A similar observation was also reported for polycarbonate.[20] The lowering of the yield strength of PBT above its glass transition temperature (T_g, about 70°C) is believed to be responsible for the sharp drop in the K_c value for the PBT samples tested at 80°C.

Figure 6 shows that a similar trend is also displayed by the PBT-CSR samples. The low K_c value at subambient temperature is rather unexpected. It is a fact that at low temperature the controlling factor in the toughening processes of rubber toughened plastics is the relaxation behavior of the rubber particles. Several studies on rubber toughened plastics indicated that toughening processes become more effective at lower temperature.[21,22] Numerous groups reported that rubber particles act as stress concentration sites to induce multiple crazing and shear yielding, thereby diffusing fracture energy throughout the matrix while decreasing the ductile–brittle transition temperature.[18,19,23,24] However, such a situation was not observed in the present PBT-CSR system. On the contrary, at −40°C the materials became more brittle with a K_c value of 2.5 MPa $m^{1/2}$. This again provides an indication that the nature of CSR modifiers plays a dominant role in determining the toughness of PBT. Judging from the plot of tan δ versus temperature for PBT and PBT-CSR shown in Figures 7 and 8, respectively, the reason behind the observed trend becomes quite clear. Apart from the prominent tan δ peak

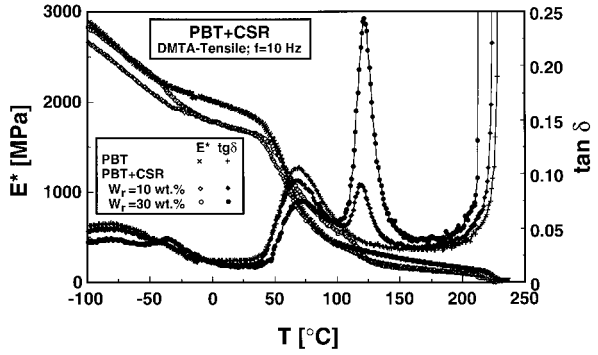

Figure 8 Variation of E^* and tan δ with temperature for PBT-CSR.

at 70°C, which is associated with the T_g of PBT, PBT-CSR also possesses another very pronounced transition peak at about 125°C. This transition is associated with that of SAN.[13] Thus, when the fracture test was conducted at ambient and subambient temperatures (i.e., well below the transition temperature of the SAN phase) the contribution from the elastomeric acrylate rubber particles (with a T_g of about −35°C, as indicated by the relatively smaller transition peak shown in Fig. 8) that form the core of the CSR is again shielded by the rigid SAN that form the shells. Thus, the CSR is likely to act as a glassy filler that has little or no significant toughening effect on the PBT matrix. Apart from that, another factor that may contribute to the embrittlement of the PBT matrix is the rubber particle size. Several studies demonstrated that the particle size of IMs plays an important role in determining the toughness of the polymer matrix.[25,26] For PBT toughened with reactive polyolefins, for instance, Deyrup et al.[27] observed that the enhancement in toughness at subambient temperatures was achieved when the mean particle size of the rubber was about 0.2 μm or less. This is obviously much smaller than the mean particle size of the CSR modifiers (i.e., 1 μm as used in the present study). In another study Brady et al.[28] reported that PBT could not be effectively toughened by the introduction of CS IMs based on butadiene rubber and *n*-butyl acrylate rubber unless these IMs were dispersed uniformly in the PBT matrix. The improvement in the degree of dispersion by the addition of dispersing or wetting agents proved to be effective in increasing the interfacial adhesion between the PBT matrix and the IM. In the case of rubber modified nylon 6,6 Wu[29–31] suggested that there is a critical interparticle distance below which ductile compositions are observed. Thus, in the present context, the inferior toughness of PBT-CSR could be attributed to several interrelated factors as stated above.

Effect of Testing Speed

As mentioned earlier, PBT suffers one major drawback in that its ductility diminishes at high deformation rates. This again proved to be the case in the present study. Table I illustrates the effect of testing speed on the fracture properties of PBT and PBT-CSR (W_r = 20 wt %). It can be seen that the fracture properties of all materials are strongly influenced by the testing speed. As the testing speed increases from 1 to 1000 mm/min the K_c values of PBT drop drastically from 5.9 to 2.2 MPa $m^{1/2}$. This may be attributed to the embrittlement of the PBT matrix under high velocity conditions. This could be expected when taking into account the viscoelastic nature of the polymeric materials whereby the segmental mobility of the polymer molecules and the plastic deformation process in the form of crazing and shear yielding are very much restricted at high deformation rates. This leads to the catastrophic failure of PBT. A similar trend can also be observed for the fracture energy G_c, albeit the drop in the values is more apparent. Similar observations were also reported for other engineering thermoplastics.[32] As for the PBT-CSR, the effectiveness of CSR rubber particles in toughening the PBT matrix is rather poor. The lower K_c value of the material (1.9 MPa $m^{1/2}$) at a testing speed of 1000 mm/min indicates that the presence of CSR tends to embrittle the PBT matrix (i.e., the rubber is behaving as a rigid filler that restrains matrix deformation). This observation coupled with the low G_c value supports our earlier results on the effect of testing temperatures.

Effect of Hygrothermal Aging

Figures 9 and 10 show the effect of immersion temperature on the K_c and G_c of PBT and PBT-

Table I Effect of Testing Speed on K_c and G_c of PBT and PBT-CSR (W_r = 20 wt %)

	K_c (MPa $m^{1/2}$)		G_c (kJ/m^2)	
	Testing Speed (mm/min)			
Material	1	1000	1	1000
PBT	5.9	2.2	20.5	5.7
PBT-CSR	3.3	1.9	7.8	5.3

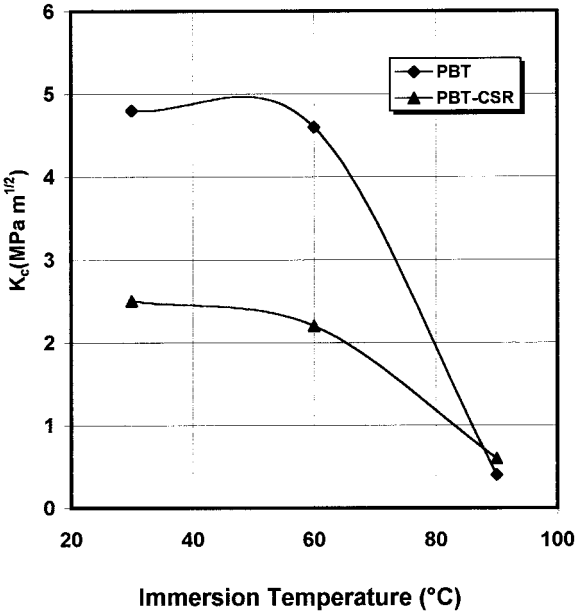

Figure 9 The effect of immersion temperatures on the K_c of PBT and PBT-CSR (W_r = 20 wt %).

CSR (W_r = 20 wt %), respectively. There is a slight drop in the K_c values of both materials upon immersion in water at 30°C (cf. the K_c data of both materials in the AR states as shown in Fig. 5). In both cases a rather small and monotonic drop in the fracture toughness was observed as the immersion temperature increased to 60°C. However, a dramatic drop in the K_c and G_c values was observed as the immersion temperature was increased to 90°C. The relative deterioration in both fracture parameters was larger in the PBT. Because PBT and PBT-CSR show similar K_c and G_c values, it becomes clear that serious embrittlement of the PBT matrix took place at a high immersion temperature.

A similar trend can also be observed from the tensile test data shown in Table II. Immersion of PBT and PBT-CSR samples in water at 90°C resulted in a dramatic reduction in the tensile strength and tensile strain values. The extremely low values suggest that both materials were fragile and incapable of supporting the external stress. This observation is in agreement with the earlier investigation conducted by Mohd Ishak and Lim.[2] A retention in tensile strength and tensile strain of about 1.5 and 3.5%, respectively, for neat PBT samples that were immersed in water at 100°C was reported. The forthcoming discussion on the mode of failure and fractography analysis reveals that hygrothermal aging at 90°C resulted in a complete change in the failure behavior of the PBT and PBT-CSR. The hydrolysis of the ester groups in the PBT is believed to operate under such an adverse condition.

Further investigation into the extent of deterioration in the fracture properties of the PBT and PBT-CSR was performed by drying these materials, which were exposed to the two most extreme immersion conditions at 30 and 90°C. The results are tabulated in Table III. The table also highlights the percentage of recovery of the derived properties with respect to the unaged or AR specimens. As expected, the tensile and fracture properties of PBT, PBT-CSR, and their related composites are not fully recovered, even after immersion in water at 30°C.

The poor recovery in the K_c and G_c values (i.e., ranging from 2.5 to 16.3%) of the PBT and PBT-CSR compared to those that were redried after immersion at 30°C (i.e., ranging from 67.9 to 86.7%) suggests that the nature of moisture attack is dependent on water temperature. At ambient temperature the interaction of water molecules with the PBT matrix is more or less physical in nature (i.e., the water is merely acting as a plasticizer) whereby upon its removal the mechanical properties of PBT and PBT-CSR are almost fully restored. This is in agreement with the earlier work of Mohd Ishak and Lim[2] on SGF-reinforced PBT composites. The poor recovery of all redried materials after immersion at 90°C clearly indicates that at a high temperature the hygrothermal aging process is no longer physical

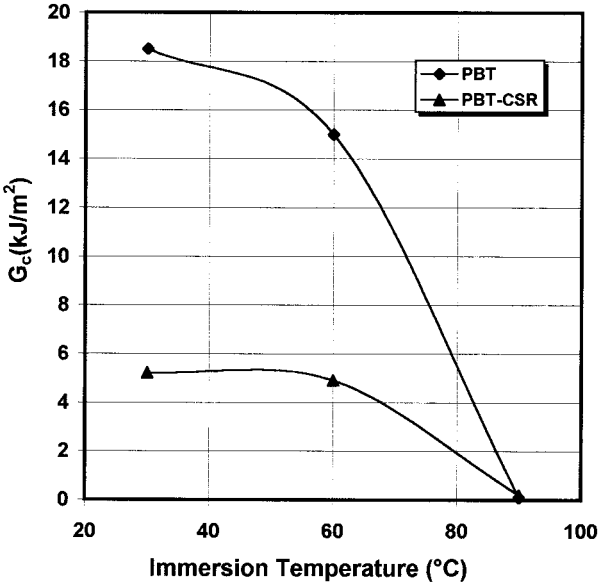

Figure 10 The effect of immersion temperatures on the G_c of PBT and PBT-CSR (W_r = 20 wt %).

Table II Tensile Properties of PBT and PBT-CSR (W_r = 20 wt %) Tested before (AR) and after Hygrothermal Aging (HA, RD)

			Aged at 30°C				Aged at 90°C			
	Unaged (AR)		HA		RD		HA		RD	
Material	Tensile Strength (MPa)	Tensile Strain (%)	Tensile Strength (MPa)	Tensile Strain (%)	Tensile Strength (MPa)	Tensile Strain (%)	Tensile Strength (MPa)	Tensile Strain (%)	Tensile Strength (MPa)	Tensile Strain (%)
PBT	55.9	8.0	50.6	16.1	54.4 (97.3)	11.4 (142.8)	11.6	0.8	19.52 (34.93)	1.1 (13.4)
PBT-CSR	43.4	6.9	38.9	5.8	43.2 (99.6)	5.3 (76.5)	14.2	1.1	26.10 (60.11)	1.5 (22.2)

The values in parentheses are the percentage recovery with respect to unaged (AR) samples. The testing conditions were 20°C and 1 mm/min.

in nature. The interaction of water molecules with the polymer matrix resulted in permanent damage to the materials. The water molecules are believed to hydrolyze the ester groups in PBT, resulting in the formation of microvoids in the samples, which would be filled with water. Upon drying, these voids will act as stress concentrators that can initiate matrix cracking, thus leading to a drastic reduction in the K_c and G_c values of the materials. The existence of these microvoids and the complete disappearance of the plastic deformation zones can be observed from the SEM micrograph of the fractured surface. This subject will be discussed in detail later. In the PBT-CSR the presence of CSR rubber particles failed to improve the PBT matrix resistance to hydrolysis.

Fractography

Figure 11(a) shows the SEM micrograph of PBT tested at room temperature at a testing speed of 1 mm/min. As expected, the usual "dimple" pattern can be observed on the fracture plane. The presence of plastic deformation in the form of matrix drawing or shear yielding [shown in Fig. 11(b)] is believed to be responsible for the ductility of the PBT matrix. Figure 12(a) demonstrates the effect of the incorporation of 10 wt % of CSR rubber on the fracture surface. The extensive plastic deformation believed to originate from rubber cavitation resulted in the formation of a modified dimple pattern on the fracture plane. The extent of fibrillation became more apparent in the PBT-CSR (20 wt % CSR) shown in Figure 12(b). In spite of the observed yielding, PBT-CSR displayed lower K_c and G_c values than that of the neat PBT. The extensive review by Walker and Collyer[25] indicated that the effectiveness of rubber particles in improving the toughness of a thermoplastic matrix is strongly controlled by its ability to act as a site to induce multiple crazing and shear yielding, thereby forming a large damage

Table III K_c and G_c Data for PBT and PBT-CSR (W_r = 20 wt %) Tested before (AR) and after Hygrothermal Aging (HA, RD)

			Aged at 30°C				Aged at 90°C			
	Unaged (AR)		HA		RD		HA		RD	
Material	K_c (MPa m$^{1/2}$)	G_c (kJ/m^2)	K_c (MPa m$^{1/2}$)	G_c (kJ/m^2)	K_c (MPa m$^{1/2}$)	G_c (kJ/m^2)	K_c (MPa m$^{1/2}$)	G_c (kJ/m^2)	K_c (MPa m$^{1/2}$)	G_c (kJ/m^2)
PBT	5.9	20.5	4.8	18.9	5.1 (86.7)	14.5 (70.6)	0.4	0.1	0.5 (7.8)	0.1 (5.8)
PBT-CSR	3.3	7.8	2.6	5.2	2.7 (80.4)	5.3 (67.9)	0.6	0.2	0.5 (16.3)	0.2 (2.5)

The values in parentheses are the percentage recovery with respect to unaged (AR) samples. The testing conditions were 20°C and 1 mm/min.

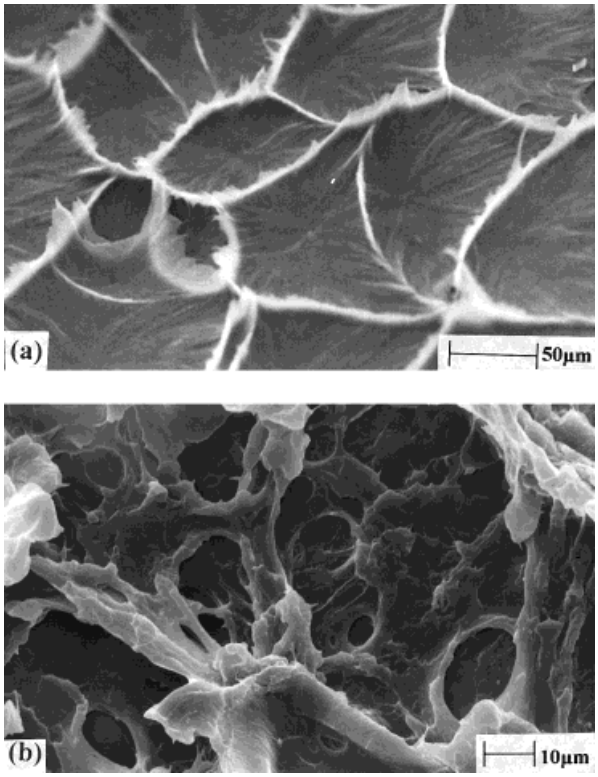

Figure 11 (a) SEM micrograph of AR PBT tested at 20°C and 1 mm/min with the presence of a "dimple" pattern on the fracture plane. (b) Plastic deformation as observed on the fracture plane of the PBT specimen tested at 20°C and 1 mm/min.

zone. In the present PBT-CSR system it is quite obvious that the existence of the various plastic deformation processes together with cavitation did not provide enough of a contribution toward the formation of an extended damage zone.

Figure 13(a,b) shows the surface appearance of PBT-CSR (20 wt % CSR) tested at −40 and 80°C, respectively. A totally different morphology can be distinguished in both cases. In the former, the ductility of the material is manifested as a limited amount of matrix tearing and fibrillation indicates that the low testing temperature has inhibited the plastic deformation process from taking place. In addition, the size of the spots (craters) surrounded by the plastically deformed matrix is beyond that of the mean CSR particle size. Thus, some of the CSR particles act as agglomerates in the cavitation process, the overall outcome of which is reduced matrix deformation and thus toughness. On the contrary, the occurrence of matrix cavitation due to CSR is more favorable at a higher testing temperature. This has resulted in the extensive fibrillation [shown in Fig. 13(b)] and stress whitening when observed normal to the specimen surface.

The appearance of the fracture surface of PBT-CSR at a much higher testing speed (1000 mm/min) is characterized by reduced plastic deformation. The overall length of the torn fibrils at a high speed fracture is less compared to that of a low speed test [compare Fig. 14 with Fig. 12(b)]. As stated earlier, the rigid shell of the CSR rubber particles and their adhesion to the matrix are believed to hinder the rubber related toughening mechanisms from providing a positive contribution toward the toughness enhancement of the PBT.

Figure 15(a,b) shows the SEM micrographs of the fracture surfaces of PBT and PBT-CSR (W_r = 20 wt %), respectively, after being subjected to hygrothermal aging at 90°C. Basically, in both cases the fracture surfaces are flat with no evidence of plastic deformation. The comparable K_c values of both materials suggest that the presence of CSR rubber particles has failed to hinder the catastrophic failure once the PBT matrix has been subjected to hygrothermal aging at high

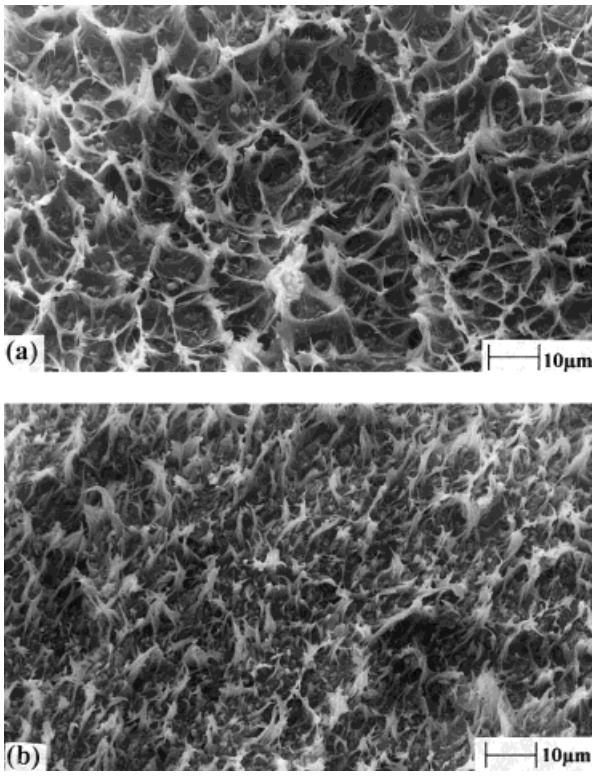

Figure 12 The effect of CSR loading on the appearance of the fracture planes for (a) PBT-CSR at 10 wt % and (b) PBT-CSR at 20 wt % tested at 20°C and 1 mm/min.

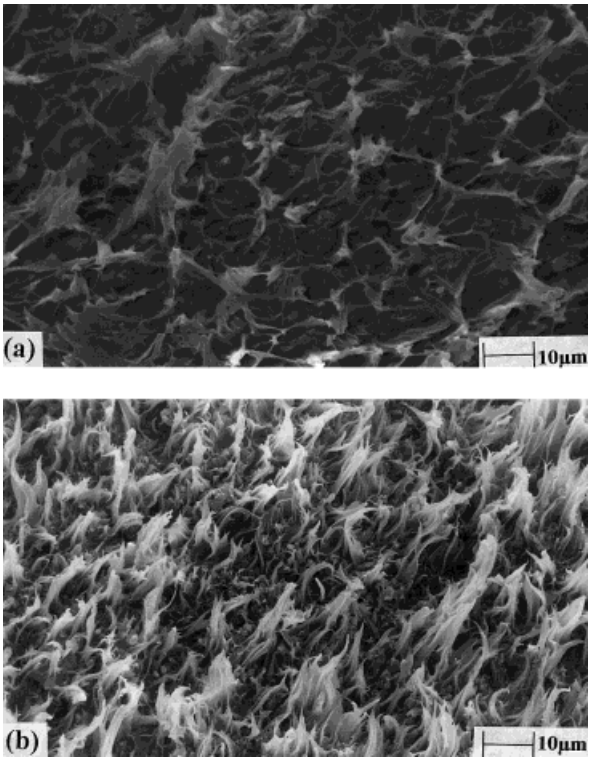

Figure 13 The appearance of the fracture surfaces of PBT-CSR (W_r = 20 wt %) tested at (a) −40 and (b) 80°C.

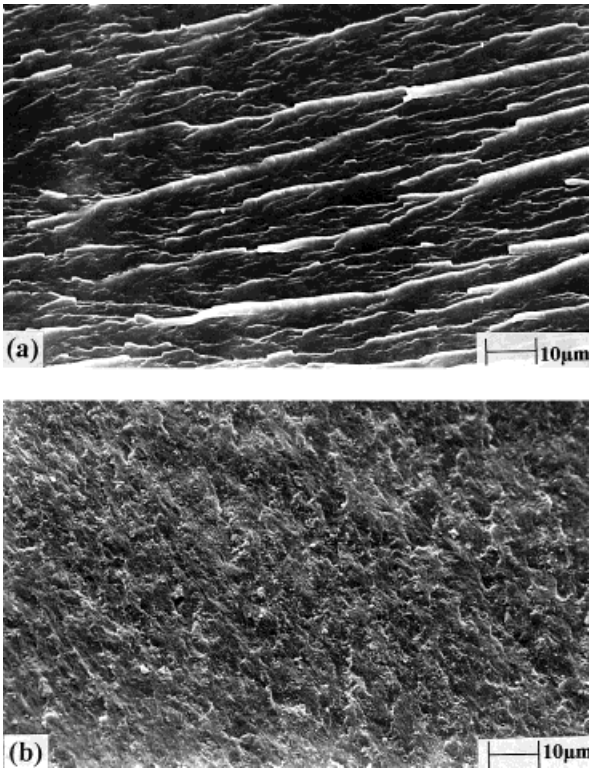

Figure 15 SEM micrographs taken on the fracture surface of (a) PBT and (b) PBT-CSR (W_r = 20 wt %) after HA at 90°C.

temperature. This explains the extremely brittle behavior of PBT and PBT-CSR during the fracture toughness test. Severe hydrolysis of the PBT matrix that leads to the formation of microvoids has been reported by Mohd Ishak and Lim.[2] Figure 16 shows that the larger CSR particles have a "salami" or "sea-islands" appearance (as indicated by the arrows). This is obvious according to the preparation of the IM (i.e., dispersion of the CS acrylate rubber in the SAN matrix). The fine structure of the CSR became visible because of the hygrothermal degradation of the dispersing SAN.

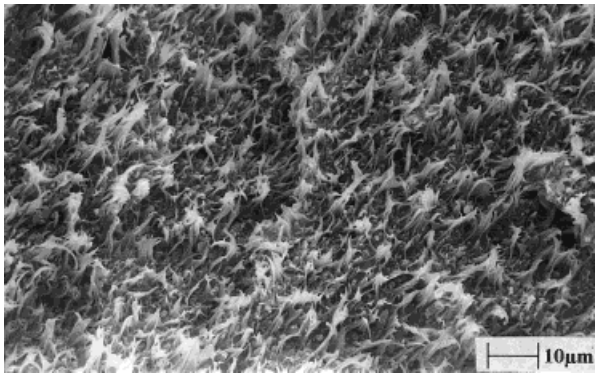

Figure 14 SEM micrograph of the appearance of AR PBT-CSR tested at 20°C and 1000 mm/min.

CONCLUSIONS

The conclusions based on this study are as follows:

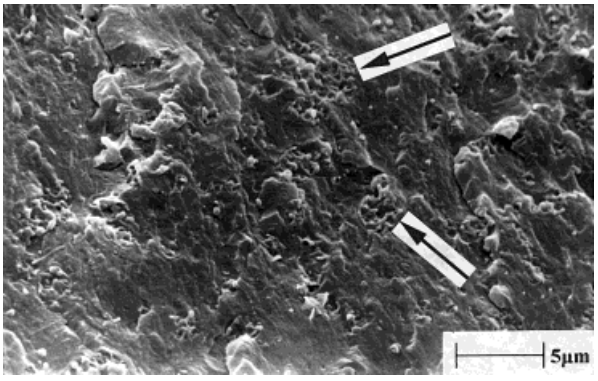

Figure 16 SEM micrograph showing "salami" or "sea-islands" features (as indicated by the arrows) of the CSR particles.

1. The fracture behavior of PBT is strongly determined by internal parameters (amount of rubber modifiers) and external parameters (testing temperature, deformation rates, and hygrothermal aging).
2. Hygrothermal aging of PBT and PBT-CSR revealed that moisture attack is either physical or chemical in nature, depending on the immersion temperature: a partially reversible physical process at ambient immersion temperature due to plasticization or an irreversible chemical process at temperatures above the T_g of the PBT due to hydrolysis.

The first author wishes to acknowledge the Marie Curie fellowship of the European Union for his stay at the IVW in Kaiserslautern and to Universiti Sains Malaysia for granting the sabbatical leave.

REFERENCES

1. Caeser, H. M. Kunstst German Plast 1987, 77, 41.
2. Mohd Ishak, Z. A.; Lim, N. C. Polym Eng Sci 1994, 34, 1645.
3. Epstein, B. N. U.S. Pat. 4,172,859, 1979.
4. Deyrup, E. J. U.S. Pat. 4,753,980, 1988.
5. Hobbs, S. Y.; Dekkers, M. E. J.; Watkins, V. H. J Mater Sci 1988, 23, 1219.
6. Hourston, D. J.; Lane, S.; Zhang, H. X. Polymer 1995, 36, 3051.
7. Hourston, D. J.; Lane, S. In Rubber Toughened Engineering Plastics; Collyer, A. A., Ed.; Chapman & Hall: London, 1994; p 243–263.
8. Kelleher, P. G.; Wentz, R. P.; Falcone, D. R. Polym Eng Sci 1982, 22, 260.
9. Golovoy, A.; Cheung, M. F.; van Oene, H. Polym Eng Sci 1988, 28, 200.
10. Czigany, T.; Mohd Ishak, Z. A.; Heitz, T.; Karger-Kocsis, J. Polym Comp 1996, 17, 900.
11. Mohd Ishak, Z. A.; Ishiaku, U. S.; Karger-Kocsis, J. In Advances in Fracture Research: Proceeding of the 9th International Conference on Fracture (ICF 9); Karihaloo, B. L.; Mai, Y.-W.; Ripley, M. I.; Ritchie, R. O., Eds.; Pergamon Press: Oxford, U.K., 1997; p 901–908.
12. Loos, A. C.; Springer, G. S. J Compos Mater 1980, 14, 143.
13. Reithel, F. J. In Engineering Plastics; Epel, J. N.; Margolis, J. M.; Newman, S.; Seymour, R. B., Eds.; ASM International: Ohio, 1988; Vol. 2.
14. Adams, R. K.; Hoeschele, G. K. In Thermoplastic Elastomers—A Comprehensive Review; Legge, N. R.; Holden, G.; Schroeder, H. E., Eds.; Hanser Publishers: Munich, 1987; p 163–196.
15. Gaymans, R. J.; Bennekom, A. J.; van Klaren, J. E. In Proceedings of the PRI Conference on Deformation and Fracture of Composites, Manchester, U.K.; 1991; paper 23.
16. Bailey, R. S.; Bader, M. G. In Proceeding of the International Conference on Composite Materials (ICCM V), San Diego, CA, 1985; p 947–951.
17. Pecorini, T. J.; Hertzberg, R. W. Polym Compos 1994, 15, 174.
18. Bucknall, C. B.; Heather, P. A.; Lazzeri, A. J Mater Sci 1989, 24, 2255.
19. Sue, H. J.; Yee, A. F. J Mater Sci 1989, 24, 1447.
20. Nielsen, L. E.; Landel, R. F. Mechanical Properties of Polymers and Composites; Marcel Dekker: New York, 1995.
21. Bucknall, C. B. Toughened Plastics; Applied Science: London, 1977.
22. Bucknall, C. B.; Street, D. G. SCI Monogr 1967, 26, 272.
23. Wu, S. J Polym Sci Polym Phys 1983, 21, 699.
24. Borggreve, R. J. M.; Gaymans, R. J.; Schuijer, J. Polymer 1989, 30, 71.
25. Walker, I.; Collyer, A. A. In Rubber Toughened Engineering Plastics; Collyer, A. A., Ed.; Chapman & Hall: London, 1994; p 29–56.
26. Borggreve, R. J. M.; Gaymans, R. J.; Schuijer, J.; Ingen Housz, A. J. Polymer 1987, 28, 1489.
27. Deyrup, E. J.; Flexman, E. A.; Howle, K. L. U.S. Pat. 4,912,167, 1990.
28. Brady, A. J.; Keskkula, H.; Paul, D. R. Polymer 1994, 35, 3665.
29. Wu, S. Polymer 1985, 26, 1855.
30. Wu, S. Polym Eng Sci 1987, 27, 335.
31. Wu, S. J Appl Polym Sci 1988, 35, 549.
32. Friedrich, K.; Karger-Kocsis, J. In Solid State Behavior of Linear Polyesters and Polyamides; Schultz, J. M.; Fakirov, S., Eds.; Prentice–Hall: Englewood Cliffs, NJ, 1990; p 249–322.